7C.9 GLOBAL DISTRIBUTION OF HOT TOWERS IN TROPICAL CYCLONES BASED ON 11-YEAR TRMM DATA

Cheng Tao* and Haiyan Jiang
Department of Earth and Environment, Florida International University, Miami, Florida

1. INTRODUCTION

Hot towers play a crucial role on the maintenance of global circulation (Yulaeva et al. 1994; Rosenlof, 1995). It is a very essential agent for heat and moisture transportation as well as mass exchange between tropopause and stratosphere (Riehl and Malkus, 1958; Simpson, J. 1990). Recent theoretical studies using satellite infrared (IR) cloud top temperature data suggest that deep convection in Tropical Cyclones (TCs) could have a major impact on the water vapor budget of the stratosphere (Rossow and Pearl, 2007; Romps and Kuang, 2009).

In the past decades, both the radar, passive microwave observations, and IR images have been used to investigate the global distribution and regional variation of deep convection in the Tropics (Petersen et al. 2001; Gettelman et al. 2004; Jiang et al. 2004; Liu and Zipser, 2005). However, since existing studies mostly focus on deep convection contributed by general convective systems, questions still remain concerning how the hot towers in TCs are distributed geographically and seasonally.

With Tropical Rainfall Measuring Mission (TRMM) satellite, the 3D rain structure can be obtained from the space-borne radar. This provides a unique opportunity to analyze the intensity of convection directly. The objective of this study is to quantitatively investigate the fractions of hot towers in TCs and its global and seasonal variation in different TC regions, intensity and intensity change stages.

2. DATA AND METHODOLOGY

The data used in this study include 11-year (January, 1998 - December, 2000 and January, 2002 - December, 2009) observations by TRMM. Considering that the quality of radar data is questionable during the orbit boost, we exclude the data from year 2001. Grouping contiguous pixels satisfying certain criteria into precipitation features (PFs), a University of Utah (UU) TRMM database has been built (Nesbitt et al. 2000; Liu et al. 2008) and successfully applied to many global and regional climatological studies (Cecil et al. 2002; Cecil et al. 2005; Zipser et al. 2006). Currently, three levels of processing of the TRMM data are constructed in the database, includeing various TRMM observed properties such as the feature size, mean rain rate, maximum 20-dBZ height, etc.

To focus on TCs specifically, a TC subset of the UU TRMM PF database upon the collaboration between Florida International University (FIU) and UU has been generated (Jiang et al. 2010). This FIU-UU TRMM TC precipitation, cloud, and convective cell feature (TCPF) database is built by interpolating the global TC best-track data into UU TRMM PF database. A TCPF is identified when the distance between TC center and the TRMM PF center is within 500 km. Besides existing TRMM observed properties in the UU TRMM PF database, a series of storm-related parameters are calculated and linearly interpolated into TRMM observation time. This contains land/ocean flag of TC center, storm 12-, 24-, 36-, and 48-h future intensity changes, etc. Furthermore, distinct TC regions, i.e., inner core (IC), inner rainband (IB), and outer rainband (OB) are sorted based on the FIU/UU TRMM TCPF database (Ramirez, 2010).

Five reference heights are selected to subjectively identify the TCPFs with overshooting tops (OTCPFs). This includes 14 km, level of NCEP reanalysis tropopause (Z_{trop}), level of potential temperature equal to 380 K calculated from NCEP sounding (Z_{380K}), level of neutral buoyancy calculated using NCEP sounding and surface equivalent potential temperature (LNB_{sfc}), and level of neutral buoyancy calculated using equivalent potential temperature at 925 and 1000 mb ($LNB_{925\&1000}$). Then the OTCPFs are found from 150,313 TCPFs when maximum 20-dBZ height observed by TRMM precipitation radar (PR) exceeds above-mentioned reference heights respectively. As a result, 1.59 % of TCPFs have 20 dBZ radar echoes at or above 14km, while only 0.09% of TCPFs are found reaching the level of 380 K.

Four overshooting parameters, i.e., overshooting distance, area, volume, and precipitating ice mass, are also calculated for each OTCPF using the same method as Liu et al. (2005). When analyzing the global distributions of the population (as shown in Fig. 1) and overshooting properties of hot towers in TCs, the results show little sensitivity to different reference levels. Therefore, in this study, the 14-km reference height is applied to examine the global and seasonal

*Corresponding author address: Cheng Tao, Dept. of Earth and Environment, Florida International University, Miami, FL 33199. E-mail: ctao003@fiu.edu

distributions of OTCPFs in different TC regions, intensity and intensity change stages.

3. Results

3.1 Global and seasonal distribution of population and overshooting properties of OTCPFs

The geographical distribution of population of total TCPFs, TCPFs without hot towers, OTCPFs, and the fraction of TCPFs contributed by hot towers are presented and compared in Figures 2a-d. Similar patterns can be seen in Figs. 2a-c, indicating that both TC and overshooting activities concentrate over northwest Pacific (NWP) basin, followed by the south Indian Ocean (SIO) and north Atlantic (ATL). However, the maximum percentage of OTCPFs is found over north Indian Ocean (NIO) basin (Fig. 2d). Averaged for basin wide, hot towers contribute, respectively, 2.10%, 1.96%, 1.66%, 1.47%, 1.20% and 1.13% of TCPFs in NIO, NWP, south Pacific (SPA), SIO, east-central Pacific (EPA), and ATL. This suggests that TCPFs located in NIO basin have a higher possibility to penetrate over 14 km.

The analysis of global distribution of overshooting properties also shows that hot towers in NIO basin has the highest percentage of OTCPFs with overshooting distance greater than 1.5 km and greatest mean overshooting distance. Two existing studies may help explain this result: 1) NIO is lack of small features with low maximum 20 dBZ echo height relative to other oceanic basins (Jiang et al. 2011); 2) mesoscale convective complexes (MCCs) are most common over the Indian subcontinent (Laing and Fritsch, 1997).

As for the seasonal variation of hot towers in TCs, it is found that monthly distributions of hot towers population as well as overshooting properties are driven by the monthly activities of TCs in each basin. For example, both the number of TCs and number of hot towers in TCs peak in September in ATL, and August in EPA.

3.2 The distribution of population and overshooting properties of OTCPFs as a function of TC regions, TC intensities, and TC intensity change stages

a. TC regions

The global distribution of fraction of TCPFs contributed by hot towers is calculated in various TC regions and presented in Figure 3a-c. Regardless of different TC basins, the TCPFs within the IC region have the highest opportunity (10.05%) to be with overshooting tops, with the IB (1.92%) and the OB (1.19%) region followed.

Figure 4a-d present the cumulative density functions (CDFs) of overshooting properties, i.e., overshooting distance, area, volume, and precipitating ice mass of OTCPFs in the IC, IB and OB region. It is observed that the largest overshooting distance (Fig. 4a), volume (Fig. 4c) and ice mass (Fig. 4d) are all found in the IC region. This is consistent with the results of previous studies that the IC region has the strongest and deepest convection compared to the IB and OB region (Cecil et al. 2002; Jiang et al. 2011). The only exception is the overshooting area (Fig. 4b), which is the greatest in the IB region globally. As for different TC basins, the result varies. That is, the largest mean overshooting area is observed in the IB for ATL, NWP, SIO and SPA while in the IC region for NIO and EPA basin. This may be due to 1) the OTCPFs in the IB region are much larger than that in the IC and OB (Jiang et al. 2011); 2) the method used in this study to separate TC regions may lead to IC contamination in IB (Ramirez 2010).

b. TC intensity stages

Similarly, the contribution of hot towers to TCPFs (in the IC region only) is calculated in various TC intensity stages, i.e., tropical depression (TD), tropical storm (TS), category 1-2 hurricane (CAT 1-2), and category 3-5 hurricanes (CAT 3-5). The percentage of OTCPFs is found to be 11.22%, 6.96%, 13.00%, and 12.41%, respectively.

Overshooting properties of OTCPFs are then investigated and tremendous discrepancies are detected between CAT 1-2 and CAT 3-5 hurricanes. The greatest mean overshooting distance, the highest percentage of overshooting distance over 1.5 km, and the largest overshooting area are all found in TS category, followed by CAT 1-2 hurricanes only slightly lower. The mean overshooting volume and ice mass are the greatest in CAT 1-2 hurricanes. CAT 3-5 hurricanes are observed to have the lowest above-mentioned overshooting properties. This may be because TCs reaching CAT 3-5 hurricanes have mostly fully developed thus a higher chance to weaken, which leads vertical convection within the IC region to decrease in this TC intensity category. In general, the relationship between the fraction and overshooting properties of hot towers and TC intensity stages is not obvious.

c. TC intensity change stages

Some previous studies suggest that hot towers in the eye region may be related to TC intensity change (Steranka et al. 1986; Simpson et al. 1998). Applying the same criteria as Ramirez (2010), identified TCPF hot towers are divided into four groups based on different TC intensity change categories. That is, OTCPFs in rapidly intensifying (RI), slowly intensifying (SI), neutral (N), and weakening (W). Globally, the opportunity for TCPFs to overshoot above 14 km is highest in RI (16.97%), with SI (10.55%), neutral (9.40%) and weakening (8.07%) following. Besides, the overshooting properties are also analyzed (in the IC region only), but no definite conclusion can be drawn from the result. This suggest that hot towers within the IC region and TC intensity change categories may be associated with each other to some

degree. However, the connection is not significant.

Considering that both RI and hot towers are very rare cases in TCs, sample size in this study may not be large enough. To clarify the exact relationship between these two and assess whether hot towers can be used as a good parameter to predict RI events, further research will need to employ several cases studies as well as modeling work.

3.3 Convective properties of OTCPFs

Four convective parameters, i.e., minimum 11 μm brightness temperature (T_{B11}), minimum 85/37 GHz Polarization Corrected Temperature (PCT), and the maximum heights of PR 40 dBZ, are selected to examine the convective properties of OTCPFs. The coefficient correlation between convective parameter and overshooting distance is found to be -0.61, -0.55, -0.52, and 0.46, respectively. As expected, the higher the overshooting top, the stronger the convection is observed. The closest association between the convective parameters and overshooting distance is found in minimum T_{B11}, which indicates the height a convective cloud can reach. This may be due to the definition of hot towers used in this study.

4. Conclusion

Globally, the TCPFs over NIO basin are found to have the highest chance to penetrate above 14 km, and they have the strongest overshooting properties. The monthly distribution of hot towers in TCs shows that such variation is driven by the activities of TCs.

Hot towers in TCs are distributed very differently in distinct TC regions. Both the highest fraction of hot towers in TCPFs and the greatest overshooting properties are observed in the IC region. The variation among different TC intensity and TC intensity change is not obvious. Results in this study suggest that hot towers in the IC region are associated with RI in TCs to some degree, since the highest fraction of TCPFs contributed by hot towers is found in RI category. However, to clearly understand the physical process of hot towers in TCs and to clarify whether hot tower can be used to better predict RI events, further study need to base on some cases studies as well as modeling work.

5. ACKNOWLEDGEMENTS

This work was supported by NASA Headquarters under the NASA Earth and Space Science Fellowship Program – Grant “NNX11AL66H”.

6. References

Cecil, D. J., and E. J. Zipser, 2002. *Mon. Wea. Rev.,* **130,** 785-801.

———, S. J. Goodman, D. J. Boccippio, E. J. Zipser, and S. W. Nesbitt, 2005. *Mon. Wea. Rev.,* **133,** 543-566.

Gettelman, A., M. L. Salby, and F. Sassi, 2002. *J. Geophys. Res., 107,* 4080, dio: 10.1029/2001JD001048.

Jiang, H., C. Liu, and E. J. Zipser, 2011. *J. Appl. Meteor. Climatol.,* **50,** 1255-1274.

———, 2011. *Mon. Wea. Rev.,* in press.

Jiang, J. H., B. Wang, K. Goya, K. Hocke, S. F. Eckermann, J. Ma, D. L. Wu, and W. G. Read, 2004. *J. Geophys. Res.,* **109,** D03111, dio: 10.1029/2003JD003756.

Laing, A. G., and J. M. Fritsch, 1997. *Meteor. Soc.,* **123,** 389-405.

Liu, C., and E. J. Zipser, 2005: *J. Geophys. Res.,* **110,** D23104, doi: 10.1029/2005JD006063.

———, ———, and S. W. Nesbitt, 2007. *Mon. Wea. Rev.,* **135,** 3086-3097.

———, ———, D. J. Cecil, S. W. Nesbitt, and S. Sherwood, 2008. *J. Appl. Meteor. Climatol.,* **47,** 2712-2728.

Nesbitt, S. W., E. J. Zipser, and D. J. Cecil, 2000. *J. Climate,* **13,** 4087-4106.

Petersen, W. A., and S. A. Rutledge, 2001. *J. Climate,* **14,** 3566-3586.

Ramirez, E. M. 2010. M. S. thesis, University of Utah, Salt Lake City, Utah, Dec. 2010.

Riehl, H., and J. S. Malkus, 1958. *Geophysica,* **6,** 503-508.

Romps, D. M., and Z. Kuang, 2009. *Geophys. Res. Lett.,* **36,** L09804, dio: 10.1029/2009GL037396.

Rosenlof, K. H., 1995. *J. Geophys. Res.,* **100,** 5173-5191.

Rossow, W. B., and C. Pearl, 2007. *Geophys. Res. Lett.,* **34,** L04803, doi: 10.1029/2006GL028635.

Simpson, J., J. B. Halverson, B. S. Ferrier, W. A. Peterson, R. H. Simpson, R. Blakeslee, and S. L. Durden, 1998. *Meteor. Atmos. Phys.,* **67,** 15-35.

Simpson, J. 1990. *Proc. Int. Symp. On Auqa and Panet,* Tokyo, Japan, Tokai University, 77-90.

Steranka J., E. B. Rodgers, and R. C. Gentry, 1986. *Mon. Weather. Rev.,* **114,** 1539-1546.

Yulaeva, E., J. R. Holton, and J. M. Wallace, 1994. *J. Atmos. Sci.,* **51,** 169-174.

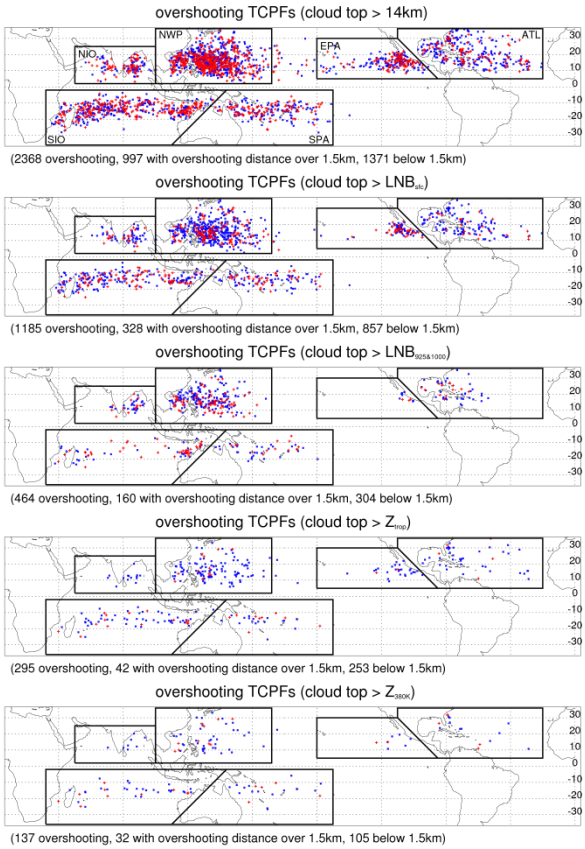

Figure 1. Location of identified overshooting TCPFs at 36oN-36oS using different reference heights. The TCPFs with overshooting distance greater than 1.5km are in red, less than 1.5km are in blue.

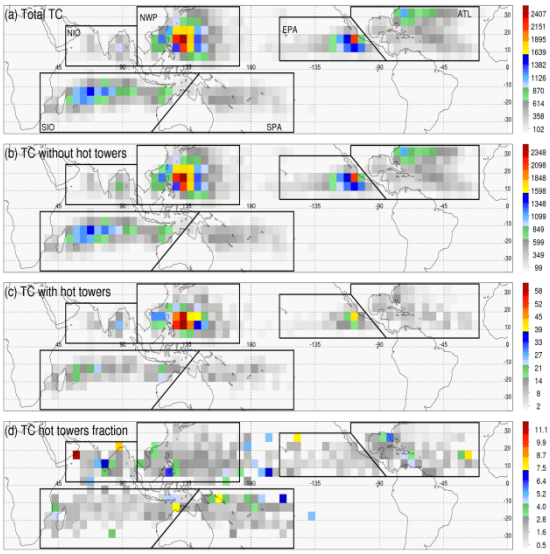

Figure 2. Global distribution of population (a) total TCPFs, (b) TCPFs without hot towers, (c) OTCPFs, (d) OTCPFs fraction (in units %) based on 5o grid for the years of 1998-2000 and 2002-09. Borders of six basins (ATL, EPA, NWP, NIO, SIO, and SPA) are indicated.

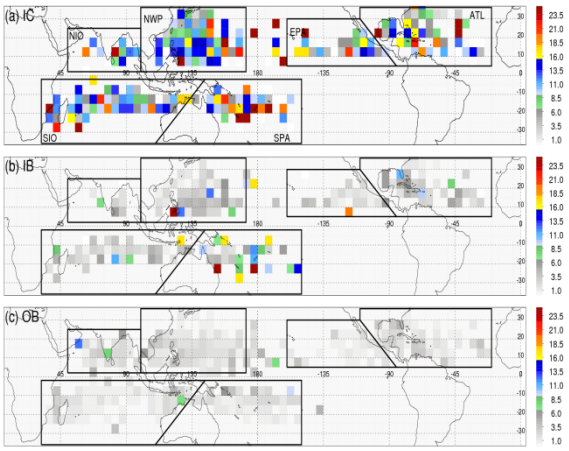

Figure 3. The TCPF overshooting fraction based on 5o grid averages in (a) IC, (b) IB, (c) OB regions for the years of 1998-2000, and 2002-09 (in units %).

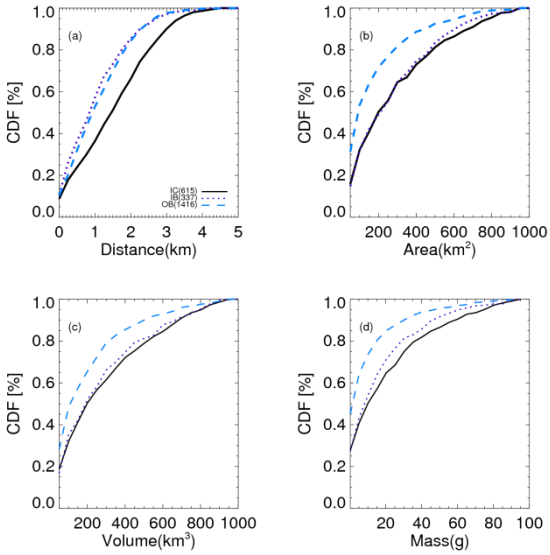

Figure 4. CDFs of (a) overshooting distance, (b) area, (c) volume, (d) ice mass for OTCPFs in IC, IB, and OB region.